

AN ADVANCED MODEL OF A HIGH PRESSURE LIQUID DIELECTRIC SWITCH FOR DIRECTED ENERGY APPLICATIONS

Joshua Leckbee, Randy Curry, and Ken McDonald

*University of Missouri - Columbia
Department of Electrical Engineering
Columbia, MO 65211*

Ray Cravey and Allen Grimmis

*Alpha-Omega Power Technologies LLC.
3701 Hawkins street NE
Albuquerque, NM 87109*

Abstract

A high power liquid dielectric switch is being developed to satisfy the requirements for future Directed Energy Applications. A flowing, high-pressure liquid dielectric was chosen for the design of a megavolt class switch operating at 100pps. This paper reports on the modeling efforts commensurate with the design of a full size, prototype 250-300kV concept validation test (CVT), switch which can transfer kilojoules per pulse. The flow system required to clear the discharge bubble and byproducts is intimately tied to the dynamics of energy deposition, and bubble formation. A circuit model has been developed to predict the discharge temporal characteristics including the voltage, current, risetime, arc energy deposition profile, time varying arc inductance, bubble formation timescales and oscillatory bubble effects. The model utilizes both the Braginskii equation and Charlie Martin's equations to calculate the energy dissipated in the arc. A comparison of the two methods is presented. An integrated model also includes the hydrodynamic equations to predict the gas bubble volume and oscillation period which are dramatically reduced with increasing pressure. Optimization studies indicate that a 1000-2000psi switch appears to have ideal attributes including minimal dielectric flow requirements, compact size and low weight for implementation of a kilojoule, rep-rate switch.

I. INTRODUCTION

Directed energy research has fueled the need for more compact switches for use in high repetition rate systems. A flowing, high pressure liquid dielectric switch is being developed to meet these needs. Liquid dielectric switches however introduce a number of complexities which will be addressed in this paper. When oil breaks down, byproducts including carbon particles and bubbles are formed. The presence of byproducts in the oil can greatly change the breakdown properties of the liquid. For a switch to recover to full voltage, the electrode gap must be free of any byproducts. The use of high pressures will decrease the gas bubble volume and subsequently reduce the amount of flow required. Flowing oil will be used to clear the byproducts out of the electrode gap between pulses.

Previous research with liquid dielectrics has shown an increase of the dielectric strength with pressure up to about 350psig [1]. This data was used in computer modeling to estimate the breakdown field of the dielectric and thus calculate the energy losses in the arc, the resistive risetime, and the gas bubble volume. As an outgrowth of the simulations and modeling, a prototype CVT switch has been built and tested to determine the dielectric strength of oil and the gas bubble characteristics at pressures up to 2000psig. Some of the modeling efforts and the preliminary results obtained using the CVT switch will be discussed, along with the experimental observations from the switch tests.

II. BUBBLE SIZE AND OSCILLATION

When an arc is formed in a liquid, chemical bonds are broken and byproducts are formed. In the case of oil, these byproducts include carbon particles and gases. Rayleigh developed equations to describe the characteristics of a bubble over time as it collapses [2]. The same equations derived to explain the collapse of a bubble have been applied to the unconstrained expansion of gas bubbles. From these equations the maximum size of the bubble and the time elapsed during one period, from formation to collapse, can be calculated. As equation (1) and figure 1 show, the maximum radius of the bubble formed increases with increasing energy lost in the arc, and decreases with increasing pressure. Equation (1) calculates the maximum bubble radius (meters) from the energy dissipated in the arc (joules) and the hydraulic pressure of the liquid (pascals). Bubbles formed due to charge injection into liquids using a point plane electrode geometry have been shown to behave as explained by Rayleigh [3]. Electrical discharges in water under vacuum have also shown agreement with Rayleigh's equations, though it was found that only about 15% of the energy dissipated in the arc was used to produce bubbles [4]. The electrodynamic behavior of the gas bubble formed from the plasma surrounding the arc is somewhat more complex than bubbles formed using explosives, due to thermal and convective losses to the electrodes. Since a fraction of the energy dissipated in the arc is used to produce bubbles, equations (1) and (2) are, we believe, a worst case approximation of bubble ra-

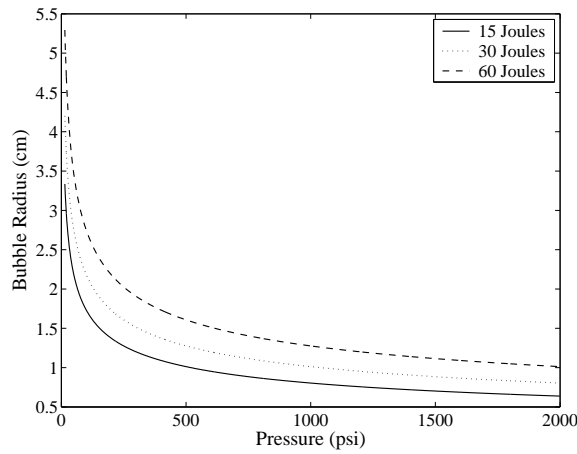


Figure 1. Plots of the maximum bubble radius versus pressure for three energy levels

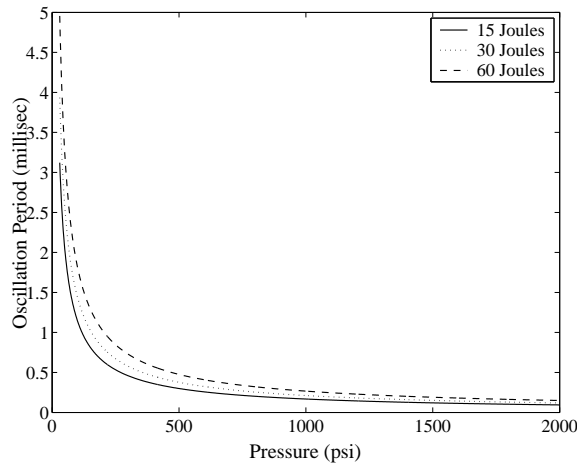


Figure 2. Plots of the oscillation period versus pressure for three energy levels

dus and volume. Experiments with underwater explosions have shown that after a bubble collapses it can rebound and go through a number of expansion and contraction cycles before going back into solution or breaking up into smaller bubbles (microbubbles). The oscillation period of the bubble, given in equation (2) and figure 2, also increases with increasing energy loss in the arc and decreases with increasing background pressure [5]. The oscillation time (seconds) is calculated from the density (kg/m^3), energy (joules), and the pressure (pascals).

$$r_{max} = \left(\frac{3 E}{4\pi P} \right)^{1/3} \quad (1)$$

$$T_{osc} = 1.135 \frac{\rho^{1/2} E^{1/3}}{P^{5/6}} \quad (2)$$

III. BREAKDOWN VOLTAGE

The breakdown voltage of a dielectric depends on a number of factors. Some of the factors which effect breakdown strength are the charge time, the electrically stressed area of electrodes, and the density of the dielectric. Work done by J. C. Martin gives an explanation of how the breakdown field strength (MV/cm) is effected by the charge time (μs) and the stressed area (cm^2) [6]. The relationship developed by Martin was modified to estimate the negative polarity breakdown field, as given in equation (3) [7]. Using equation (3), the breakdown field for a 3.8cm (1.5in) hemispherical electrode and a 0.2cm gap is 1MV/cm. Previous work on the breakdown of liquid dielectrics under pressure shows that as pressure increases, the breakdown strength increases for small electrode areas. Kao also reported that transformer oil pressurized up to about 350psig showed a gain in the breakdown strength of up to 35-40%, over those at atmospheric pressure [1]. Based on this information, we expected approximately a 35-40% increase in the dielectric strength of oil at 2000psig. However, the experimental data showed a gain of only 20-25%.

$$E_{br} = 1.41 \left(\frac{.48}{t_{eff}^{1/3} A^{.075}} \right) \left[1 + .12 \left(\frac{E_{max}}{E_{mean}} - 1 \right)^{1/2} \right] \quad (3)$$

IV. SWITCH ENERGY LOSS

The integrated switch model must estimate switch losses to calculate bubble radius. The switch loss can be obtained using J. C. Martin's equation for switch loss, equation (4). In this equation, the energy loss (joules) is calculated from the peak voltage (kV), the driving impedance (Ω) and the resistive rise time (μs). The equation for resistive rise time, equation (5), can be used to calculate the exponential resistive phase transition time (ns), given the driving impedance and the breakdown field strength (MV/cm). Calculations of the CVT switch loss based on equation (4) and a charge voltage of 250kV predict an energy loss of about 37J. As shown in figure 1 and figure 2, the bubble radius is bounded as a function of the arc loss from 15-60J. The energy loss calculation is approximate and has not been verified in the high pressure regime of interest. Thus it may vary as much as 30-40%.

$$E = \left(\frac{V^2}{4Z} \right) \tau_r \quad (4)$$

$$\tau_r = \frac{5}{Z^{1/3} E_{br}^{4/3}} \quad (5)$$

The change in voltage across a switch can be described using the equations for resistive rise time, inductive rise time, and total rise time. During the resistive rise time, the arc is formed and the resistance of the arc decreases rapidly from an open circuit to an impedance much

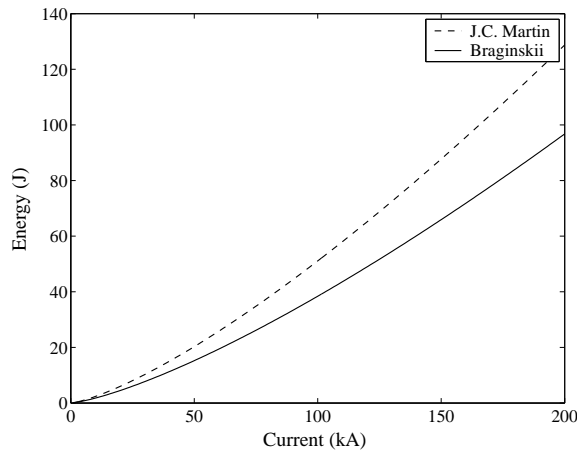


Figure 3. Comparison of the J. C. Martin energy loss approximation to the Braginskii loss method for a range of currents.

less than the driving impedance. The inductive rise time follows the resistive rise time and describes the time while the arc is expanding, and the inductance is decreasing. The total rise time, shown in equation (7), gives the time for the voltage across the switch to decrease from 90% to only 10% of the peak value. Based on these equations, the CVT switch with a charge voltage of 250kV is expected to have a 10%-90% inductive and resistive rise time of 10-11ns.

$$\tau_L = \frac{L}{Z} \quad (6)$$

$$\tau_{total} = 2.2\tau_r + 2.2\tau_L \quad (7)$$

The switch loss can also be calculated from the current through the switch and the time varying arc resistance obtained using Braginskii's formula, equation (8). The resistance is obtained using equation (8), which describes the time varying arc radius, and assuming a constant conductivity, as described by Tom Martin [8] [9]. The equation for the time varying arc radius determines the radius (cm) from the density of the dielectric (g/cm^3), the current (kA), and the time (μs). Using this method to calculate the energy loss in the switch, one only needs to know the current through the switch, the length of the electrode gap and the conductivity of the arc. Using Tom Martins assumption of a conductivity of 600(1/ohm-cm), and the anticipated current though the CVT switch, the energy loss is about 30J or 33% less than that estimated by Martin's formulae.

$$r = 0.093\rho^{-1/6}I^{1/3}t^{1/2} \quad (8)$$

Both methods of calculating the energy are intended as an approximation. A comparison of the two methods of energy calculation has been made with respect to current through the switch (see figure 3). The equation derived by

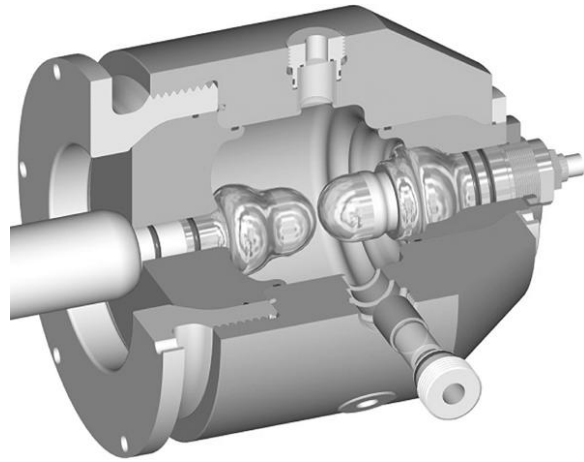


Figure 4. Cross section of the CVT switch with hemispherical electrodes, view ports, and oil ports.

Braginskii for an arc formed in air, equation (8), was used for the comparison. A comparison to experimental data is necessary to determine which method is most accurate for a particular experimental setup. However, it is interesting to note that the curves overlay within a few percent if the Braginskii equation is multiplied by 1.33.

V. EXPERIMENTAL PROGRAM AND CVT SWITCH DESIGN

The switch shown in figure 4 was integrated into the single shot test stand as shown in figure 5. The circuit consisted of two capacitors, each $1.85\mu F$, charged to opposite voltages and then switched into the primary of a 1:5 step up transformer. The system pulse charges the 1.6Ω water transmission line to 250-300kV in 1-1.2 μs with a $t_{effective}$ of 0.5 μs , producing a 100ns pulse when discharged. A short oil transmission line was used to connect the larger water transmission line to the smaller diameter output switch. The load resistor is embedded in the short oil section between the water line and the output switch. The oil section and load resistor are shown in figure 5 as a resistor.

Three electrical diagnostics were used to monitor the voltage and current. A Rogowski coil was used to measure the current, and two \dot{D} probes were used to measure voltage. One \dot{D} probe is located in the water transmission line, and the other was placed in the short oil section between the load resistor and the output switch. Both were calibrated with an external Tektronix 6015 probe and a Pearson current monitor. The optical diagnostics were as described in a separate conference paper [10].

VI. CIRCUIT SIMULATION

The CVT test circuit, as described above, was modeled using PSpice. The circuit was simulated using a discrete

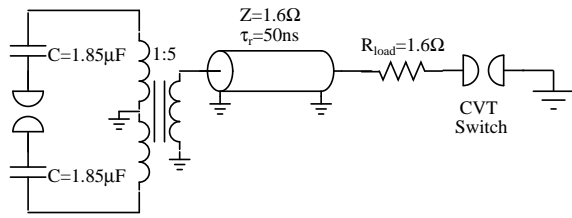


Figure 5. Single shot experimental test circuit for CVT switch

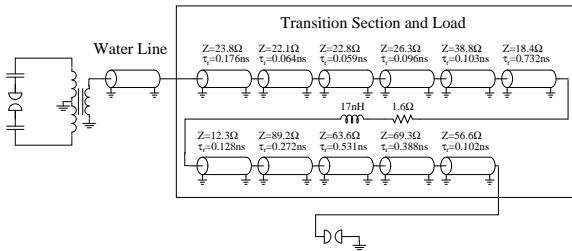


Figure 6. Transmission line model used to simulate the risetime of the circuit

transmission line approximation of the 1.6Ω water line, load resistor, transition section, and CVT switch. The transmission line model is shown in figure 6 and consists of 11 transmission line sections. The oil transition section was modeled as both a transmission line section and as a discrete LC network. Both models gave excellent results. The discrete LC network model is compared to experimental data in figure 7. The calculated risetime of the circuit was 100ns with the switch transition section and the inductance of the load included. The 10-11ns risetime of the switch was used for the simulations. The simulated voltage characteristics accurately match the \dot{D} probe signals. The energy loss into the arc has not yet been measured and will be measured in future experiments.

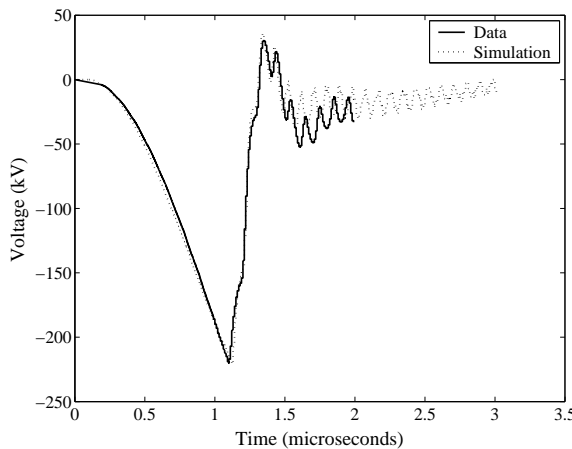


Figure 7. Comparison of voltage data to circuit simulations.

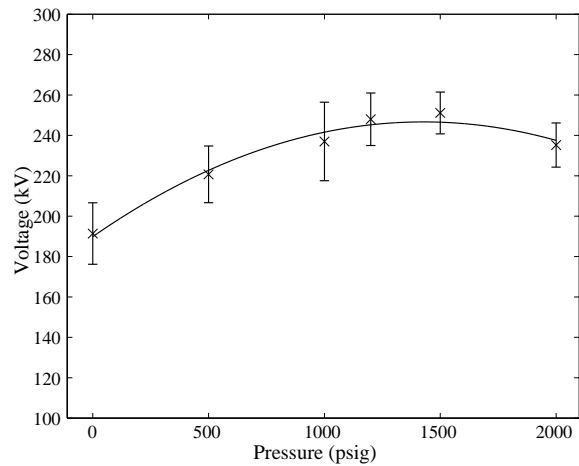


Figure 8. This plot shows the average breakdown voltage for a 0.2cm gap at various pressures with one standard deviation error bars.

VII. BREAKDOWN VS. PRESSURE

Experiments have shown that pressurizing a dielectric increases its breakdown strength. Experiments were run using 3.81cm (1.5in) diameter hemispherical shaped electrodes and a gap spacing of 0.2cm. The results of these experiments are plotted in figure 8. Each data point represents an average of 10 pulses for a given pressure. The error bars represent one standard deviation for the set of data at that pressure and the curve fit is a second order polynomial least-squares approximation. The data shows that the breakdown strength increases by about 25-30% as pressure increases from atmospheric pressure to 1500psig. The breakdown strength then decreases slightly for increasing pressures, with an overall gain of only 23% at 2000psig. This is much less than the 40% gain expected from extrapolating Kao's data out to higher pressures. The unconditioned electrodes had a statistical deviation of $\pm 10\%$, which decreased to $\pm 6.5\%$ after 45 conditioning shots.

VIII. BREAKDOWN BYPRODUCTS

The maximum radius of the bubbles formed at atmospheric pressure could not be determined because of the limited field of view. The 1.31cm optical port in the switch housing provided a field of view of about 2cm in diameter. Theoretical calculations predict, that at atmospheric pressure, the maximum bubble radius would be about 4cm and thus much too large to be seen in the photographs. Due to the geometrical restriction of the electrodes, the bubbles are not allowed to expand equally in all directions, as a result the bubbles break up into smaller bubbles instead of oscillating.

It was found that at high pressures, above 500psig, the equations overestimate the size of the bubbles formed. At

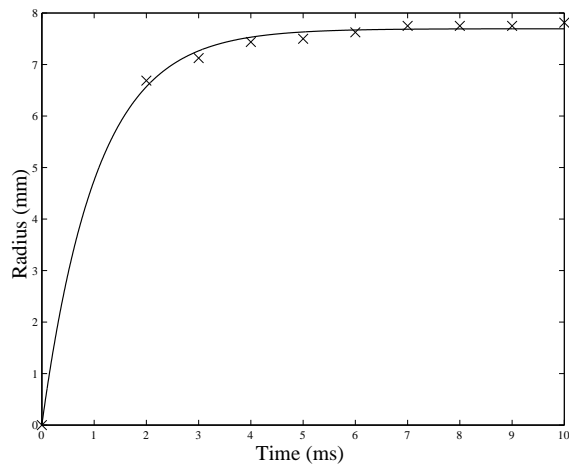


Figure 9. This plot shows the radius of a carbon cloud formed at 2000psig as a function of time.

1000psig, a switch dissipating 15-60J of energy would be expected to form bubbles with diameter around 2cm and an oscillation period of less than 1ms. Photographs have shown that the bubbles observed late time are less than 1mm in diameter, and some appear to be reabsorbed into solution after 20ms. The bubble formation was occluded by the carbon cloud expansion and was not resolved. At the higher pressures, the formation of a single bubble was not found. The equations used to predict bubble dynamics indicate that for an energy deposition of 15-60J in oil at 1500psig, bubbles of about 1cm diameter should be produced. Photographs indicate that bubbles formed at and above this pressure are much smaller, and quickly break up into microbubbles. The physics of this phenomena has not yet been explained.

As pressure increases, the formation of carbon is more localized. At atmospheric pressure, some carbon is produced, but the amount is either small enough that it is not visible in photographs or the expanding bubble wall disperses the carbon out of the electrode gap. At 500psig, enough carbon is produced to be visible as a cloud. At higher pressures, the carbon is seen in photographs as a dense cloud. As with the formation of bubbles, it is likely that the formation of carbon is also a function of energy dissipated in the arc. Experiments are under way to measure the amount of carbon produced.

The expansion of the carbon clouds is much slower than that of the bubbles formed in the high pressure regime. Measurements of bubbles formed at atmospheric pressure showed initial expansion velocities of about 25m/s. Expansion of carbon clouds is very slow in comparison. Figure 9 shows that while the initial expansion can be 3-5m/s, the

expansion slows to less than 12.5cm/s after about 2ms. For a flowing oil switch, where the oil will sweep the byproducts out of the electrode gap, the slowly expanding carbon cloud lowers the flow required for recovery of the voltage holdoff. Calculations indicate that a 1-2l/s flow will be required for 100-200pps operation of a switch transferring kilojoules per pulse.

IX. SUMMARY

We are currently in the process of measuring the arc loss and the amount of carbon being produced by the switch at atmospheric pressure and in the 6.89-13.8MPa (1000-2000psi) range. Once the carbon formation is measured, the amount of material ionized can be estimated. This will provide a cross correlation to the switch model. The model which integrates the switch loss with the hydrodynamic equations will be refined and will be compared to the arc loss measurements. In parallel a repetitive switch that will transfer 250-300J per pulse is under construction and will be integrated with a rep-rate test stand [11]. Diagnostics will be integrated into the test stand that will measure the switch current and the voltage drop across the switch. This will allow the energy loss calculations to be verified.

X. REFERENCES

- [1] K. C. Koa and J. B. Higham, "The effects of hydrostatic pressure, temperature, and voltage duration on the electric strength of hydrocarbon liquids," *J. Electrochem. Soc.*, vol. 108, pp. 522-528, 1961.
- [2] J. W. Strutt and Rayleigh, "On the pressure developed in a liquid during the collapse of a spherical cavity," *Phil. Mag.*, vol. 34, pp. 94-98, 1917.
- [3] R. Kattan, A. Denat, and N. Bonifaci, "Formation of vapor bubbles in non-polar liquids initiated by current pulses," *IEEE Trans. Elect. Insulation*, vol. 26, pp. 656-662, 1991.
- [4] G. L. Chahine, G. S. Frederick, C. J. Lambrecht, G. S. Harris, and H. U. Mair, "Spark-generated bubbles as laboratory-scale models of underwater explosions and their use for validation of simulation tools," in *SAVIAC Proc. Shock and Vibrations Symp.*, vol. 2, Nov 1995, pp. 265-276.
- [5] H. F. Willis, "Underwater explosions," *British Rep. WA-47-21*, 1941.
- [6] J. C. Martin, "Nanosecond pulse techniques," *Proc. IEEE*, vol. 80, no. 6, pp. 934-945, 1992.
- [7] R. J. Adler, "Pulse power formulary," North Star Research Corp., June 2002.
- [8] S. I. Braginskii, "Theory of the development of a spark channel," *Soviet Physics JETP*, vol. 7, no. 6, pp. 1068-1074, Dec 1958.
- [9] T. H. Martin, J. F. Seamen, and D. O. Jobe, "Energy losses in switches," in *Proc. IEEE 9th Int. Pulsed Power Conf.*, vol. 1, 1993, pp. 463-470.
- [10] R. Curry, K. McDonald, *et al.*, "Development of high power, high pressure, rep-rate, liquid dielectric switches," in *IEEE 14th International Pulsed Power Conference*, 2003.
- [11] P. Norgard, R. Curry, and K. McDonald, "A high pressure, rep-rate, liquid dielectric switch test-stand," in *IEEE 14th International Pulsed Power Conference*, 2003.